Journal of
Composites Science

MDPI

Article

Ready-to-Use Recycled Carbon Fibres Decorated with Magnetic Nanoparticles: Functionalization after Recycling Process Using Supercritical Fluid Chemistry

Sophie Martin [1,*], Tatjana Kosanovic Milickovic [2], Costas A. Charitidis [2] and Sandy Moisan [1]

[1] IRT Jules Verne, Nantes Université, F-44000 Nantes, France
[2] Research Lab of Advanced, Composite, Nanomaterials and Nanotechnology (R-NanoLab), School of Chemical Engineering, National Technical University of Athens, 9 Heroon Polytechniou St., Zographos, 15773 Athens, Greece; tkosanovic@chemeng.ntua.gr (T.K.M.); charitidis@chemeng.ntua.gr (C.A.C.)
* Correspondence: sophie.martin@irt-jules-verne.fr

Abstract: An innovative simultaneous process, using supercritical fluid (SCF) chemistry, was used to recycle uncured prepregs and to functionalize the recovered carbon fibres with Fe_3O_4 magnetic nanoparticles (MNPs), to produce a new type of secondary raw material suitable for composite applications. This specific functionalization allows the fibres to be heated by induction through a hysteresis loss mechanism characteristic for nanoparticle susceptor-embedded systems, for triggered healing properties and a potentially easy route for CF reclamation. Using SCF and hydrothermal conditions for recycling, functionalization of fibres can be performed in the same reactor, resulting in the creation of ready-to-use fibres and limiting the use organic solvent. After cutting the uncured prepreg to the desired length to fit in future applications, supercritical CO_2 extraction is performed to partially remove some components of the uncured prepreg matrix (step 1). Then, the recycled carbon fibres (rCFs), still embedded inside the remaining organic matrix, are brought into contact with reactants for the functionalization step (step 2). Two possibilities were studied: the direct synthesis of MNPs coated with PAA in hydrothermal conditions, and the deposition of already synthesized MNPs assisted by supercritical CO_2-acetone. No CF surface activation is needed thanks to the presence of functional groups due to the remaining matrix. After functionalization, ready-to-use material with homogeneous depositions of MNPs at the surface of rCF is produced, with a strong magnetic behaviour and without observed degradation of the fibres.

Keywords: supercritical fluid chemistry; recycling; carbon fibres; functionalization; magnetic nanoparticles; hysteresis heating

check for updates

Citation: Martin, S.; Milickovic, T.K.; Charitidis, C.A.; Moisan, S. Ready-to-Use Recycled Carbon Fibres Decorated with Magnetic Nanoparticles: Functionalization after Recycling Process Using Supercritical Fluid Chemistry. *J. Compos. Sci.* **2023**, *7*, 236. https://doi.org/10.3390/jcs7060236

Academic Editor: Francesco Tornabene

Received: 6 May 2023
Revised: 26 May 2023
Accepted: 31 May 2023
Published: 6 June 2023

1. Introduction

Carbon fibre (CF) is an ideal reinforcement for polymer matrix composites due to its excellent high specific strength, light weight, and outstanding thermal properties. Due to the high cost, recycling strategies are under development for its recovery [1]. Recently, an innovative process for recycling uncured prepreg sheets made of CF and epoxy resin was elaborated for obtaining recycled CF at IRT Jules Verne [2]. This recycling process involved sc-CO_2 for extracting partially bisphenol A/F and aminophenol. This new type of secondary raw material possesses the great advantage of not being tacky compared to fresh uncured material, with the capability to control CF length.

One way to reuse rCF is in the production of thermoplastic (TP) compounds for 3D printing feedstock, in form of pellets or filaments, depending on the requirements of targeted additive manufacturing (AM) technology. To design a more sustainable semi-product, the deposition of magnetic nanoparticles (MNPs) at the rCF surface is identified to bring induced, through hysteresis loss mechanism in an alternating magnetic field, healing properties and improve the recycling of the new composite structure by applying a magnetic field [3]. The magnetic field induces a local heating and a swelling of TP around the fibres, allowing crack reparation or CF recovery [4–6]. Following the work of Hergt et al. [7], Fe_3O_4 NPs with a main diameter of 20 nm seem to be optimal for insuring good magnetic properties for heating applications. To efficiently functionalize CF with Fe_3O_4, two options can be considered: (i) in situ Fe_3O_4 NP synthesis and deposition in the presence of rCF, or (ii) deposition of stabilized Fe_3O_4 NPs on the CF surface. As functionalization should be done after the recycling process, the objective is to use supercritical media for this step as well, limiting the use of organic and/or toxic solvents.

For the synthesis of Fe_3O_4 with a size of 20 nm, hydrothermal conditions are mainly used. For instance, Mizutani et al. [8] reported a one-step hydrothermal process to prepare highly crystalline 10 to 40 nm Fe_3O_4 nanopowders without using the surfactants. The same procedure is described by Haw et al. [9], Kolen'ko et al. [10], and Kumar et al. [11], with the addition of chitosan, poly(acrylic acid) (PAA) and polyethylene glycol 400 (PEG-400) leading to a more homogeneous distribution in size of 17 nm, 20 nm and 27 nm, respectively. Sc-CO_2 can also be used to synthesize magnetic nanoparticles [12]. $Fe(NO_3)_3$ ethanol solution is expended in a batch supercritical reactor by introducing sc-CO_2 to form a homogeneous fluid. The key role of sc-CO_2 is to allow an optimal impregnation of graphene foam followed by homogenized nucleation of Fe_3O_4 NPs, confirmed by the obtained homogeneous Fe_3O_4 coating.

A similar approach for the functionalization of carbon nanotubes with Fe_3O_4 NP has been reported [13–15]. Functional groups (-OH, -COOH or -NH) seem essential to serve as anchor points for the attachment of Fe ions during precursor dissolution via Van der Waal's forces [16]. Synthesis of Fe_3O_4 in sc-CO_2 to functionalize carbon is reported in the literature mostly for battery storage, to create alternative negative electrode materials [12,17]. Hu et al. [12] described a synthesis of Fe_3O_4 into a graphene foam with a diameter of 11 nm without surfactant. Wang et al. [17] synthesized 14 nm Fe_3O_4 anchored into a 3D-carbon network. Moreover, SCF is used for the impregnation of polymers with nanoparticles for pharmaceutical uses: for example, sodium valproate nanoparticles were loaded on polyvinylpyrrolidone (PVP) and hypromellose (HPMC) polymers [13–15].

To the best of our knowledge, direct synthesis of MNPs, or deposition of already synthesized MNPs, has not been performed to functionalize CFs. In the present work, the functionalization trials of CF with MNP are performed using two approaches: (i) using hydrothermal synthesis of MNPs in the presence of carbon fibres, and (ii) with sc-CO_2 synthesis. Several supercritical fluid chemistry strategies are tested to define the best rCF functionalization approach with Fe_3O_4 NPs after the sc-CO_2 extraction process to obtain ready-to-use fibres.

2. Materials and Methods

2.1. Materials

Reclaimed carbon fibres (rCFs) were provided from the prepreg recycling process developed previously with sc-CO_2 [3] (see Figure 1). The epoxy matrix is partially removed from prepregs by dissolution in sc-CO_2; however, a part of epoxy is still present on the material. The composite "rCF" is composed of 68% wt CF, and 32% wt is the remaining epoxy matrix. Samples are cut into two dimensions: the shorts are 15 × 15 mm for the first synthesis, and the longs are 12.5 × 80 mm for induction tests with two different experimental set-ups.

Precursors and reactants were reagent grade with a minimum purity of 99% and were purchased from Sigma Aldrich (Saint Quentin Fallavier, France) (: $FeCl_3$, $FeSO_4{\cdot}H_2O$, $FeCl_2{\cdot}4H_2O$, PEG-400, PAA, $Fe(NO_3)_3{\cdot}9H_2O$; they were used with no further purification. From aqueous solutions, hydrogen peroxide (H_2O_2, 35 wt%), sodium hydroxide (NaOH, 1M) and ammonium hydroxide (NH_4OH, 28 wt%) were used. The solvents used were reagent grade absolute ethanol and acetone, purchased from Sigma Aldrich (Saint Quentin Fallavier, France). The nanoparticles used for deposition are Fe_3O_4 NP capped with oleic acid, with a size of 20 nm, synthetized by NTUA with coprecipitation of ferric salts. These particles were selected based on their magnetic properties, recorded using the Superconducting Quantum Interference Device (SQUID) [18]. The results obtained on Moment versus Applied field @ 300 K and Moment versus Temperature @ H = 100 Oe for synthesized magnetite Fe_3O_4 nanoparticles were comparable to the results found in the literature for MNPs prepared by the co-precipitation method [19]. In addition, their magnetic behaviour was evaluated until 900 K, and magnetic behaviour plots—mass magnetization ($A \cdot m^2/kg$) versus magnetic field (A/m) and mass magnetization ($A \cdot m^2/kg$) versus temperature (K)—were recorded. Symmetric hysteresis and saturation magnetization was observed for the analysed Fe_3O_4 nanoparticles showing ferrimagnetic behaviour having a saturation magnetization of 45 $A \cdot m^2/kg$; this is obviously lower than that of the bulk Fe_3O_4 (90 $em\mu \cdot g^{-1}$) [20] and may be attributed to the small particle size effect, since a noncollinear spin arrangement occurs primarily at or near the surface, which results in the reduction of magnetic moment in Fe_3O_4 NPs [21,22]. The Curie temperature was verified at 836 K [23]. Polypropylene used for impregnation of functionalized rCFs for induction heating experiments was purchased from Sigma Aldrich (Burghausen, Germany) (Isotactic, average Mw, 250,000).

Figure 1. Photography of rCF produced after sc-CO_2 extraction of uncured UD-prepreg [2]. Brown sheets are the paper peeled off the rCF.

2.2. Methods

2.2.1. CF Extraction and Functionalization in sc-CO_2 Conditions

CF extraction was performed in an sc-CO_2 batch extractor made of stainless steel, with an internal reactor volume of 7 L, a maximum working pressure of 30 MPa, and a maximum working temperature of 200 °C. UD-prepregs were placed in a basket, which was inserted subsequently into the batch reactor. Sc-CO_2 was injected inside the reactor, and an organic phase mainly composed of bisphenol A and F and aminophenol was extracted from the prepregs. At the end of extraction, the UD-prepregs became rCF.

For the functionalization phase, the solution containing precursors (for CF-sc-CO_2) or MNP (for CF-dep-acetone and CF-dep-EtOH) was injected in the still-closed reactor containing rCF, and the conditions of pressure and temperature were set to obtain the required functionalization reactions. After the CF treatment step, functionalized rCF was recovered from the reactor, and after a manual separation from paper sheets, it was ready for compounding or reuse [2]. In particular, the following series of CF functionalization experiments was performed (see Table 1):

- sc-CO_2 assisted MNP synthesis on CFs (sample ID: CF-sc-CO_2): rCF was placed in the reactor, then a solution of $Fe(NO_3)_3 \cdot 9H_2O$ (7.89 g) was added to absolute ethanol (800 mL). After sealing of the reactor, CO_2 was added at 9 MPa at 45 °C; then, the system was heated at 120 °C for 9 h. After cooling of the reactor to room temperature, CFs were separated, washed 5 times with absolute ethanol and dried at 80 °C for 12 h.

- deposition of MNPs at the CF surface in acetone media (sample ID: CF-dep-acetone (and -long)): rCFs (0.50 g) (short and long) were placed in the reactor, and MNPs (0.25 g of Fe_3O_4) dispersed in acetone (50 mL) were added. The reactor was sealed, CO_2 was added and the system was heated at 70 °C for 1 h under pressure of 11 MPa. After cooling of the reactor to room temperature, CFs were separated, washed 5 times with absolute ethanol and dried at 70 °C for 12 h.
- deposition of MNPs at the CF surface in ethanol media (sample ID: CF-dep-EtOH): rCFs (0.50 g) were placed in the reactor, and MNPs (0.25 g) dispersed in absolute ethanol (50 mL) were added. The reactor was sealed, CO_2 was added, and the reactor was heated at 50 °C for 1 h under pressure of 30 MPa. After cooling of the reactor to room temperature, CFs were separated, washed 5 times with absolute ethanol and dried at 70 °C for 12 h.

Table 1. Summary of experiments.

Sample ID	Type of Experiment	Precursors or MNP	Reactant	Coating	Solvents	Ref.
CF-hydro-nocoating	hydrothermal/synthesis	$FeCl_3$ and $FeSO_4\cdot7H_2O$	NaOH	/	Water	[8]
CF-hydro-PAA (and -long)	hydrothermal/synthesis	$FeCl_2\cdot4H_2O$ and $FeCl_3\cdot6H_2O$	Ammonia	PAA	Water	[10]
CF-hydro-NaOleate	hydrothermal/synthesis	$FeCl_2\cdot4H_2O$ and $FeCl_3\cdot6H_2O$	Ammonia	Sodium oleate	Water	[10]
CF-hydro-PEG	hydrothermal/synthesis	$FeCl_2\cdot4H_2O$ and $FeCl_3\cdot6H_2O$	NaOH	PEG-400	Water And Ethanol	[11]
CF-sc-CO_2	sc-CO_2/synthesis	$Fe(NO_3)_3\cdot9H_2O$	/	/	Ethanol	[12]
CF-dep-acetone (and -long)	sc-CO_2/deposition	Fe_3O_4@oleic-acid	/	/	Acetone	[13–15]
CF-dep-EtOH	sc-CO_2/deposition	Fe_3O_4@oleic-acid	/	/	Ethanol	[13–15]

2.2.2. CF Functionalization (Synthesis and Deposition of MNPs) in sc-H_2O Conditions

A supercritical water batch reactor with a reactor volume of 2 L was used for hydrothermal conditions, with a maximum working temperature of 500 °C and pressure of 30 MPa [24]. For technical reasons, experiments were not performed in the same reactor as for sc-CO_2. The authors assumed that this would not affect the results. The solution containing precursors and rCFs was added to the reactor, heated to the required temperature, and for the hydrothermal reaction, autogenous pressure was generated with a liquid/gas phase change of water. Different capping agents were added as stabilizers to inhibit the over-growth of nanoparticles and prevent their aggregation/coagulation in colloidal synthesis. For SC synthesis or deposition, pressure was adjusted by a pumping system [25]. Pressure and temperature gauges were connected to the reactor, and a rupture disk was positioned to protect the reactor from pressures greater than the design pressure and for safety reasons. Depending on the reaction, the system was maintained during the required time, and the reactor was cooled, to regain atmospheric pressure and temperature. Specifically, the following hydrothermal coprecipitation trials for Fe_3O_4 synthesis with CF were carried out:

- Without a capping agent (sample ID: CF-hydro-nocoating): rCFs were placed in the reactor, and 400 mL of aqueous solution of $FeCl_3$ (3.244 g) and $FeSO_4\cdot7H_2O$ (2.78 g) were added. The reactor was sealed, the air was purged by N_2, and the system was heated at 200 °C for 1 h. NaOH 1M (200 mL) was added drop-by-drop in the N_2 atmosphere. After cooling of the reactor to room temperature, CFs were separated, washed 5 times with deionized water and dried for 12 h at 80 °C.
- In the presence of a PAA capping agent (sample IDs: CF-hydro-PAA (and -long)): rCF (short and long) were placed in a reactor, and a solution of $FeCl_2\cdot4H_2O$ (15.8 g) and $FeCl_3\cdot6H_2O$ (37.8 g) in 70 mL of deionized and deoxygenated water (N_2 purged) was added. Subsequently, ammonia solution (28%, 150 g) was added, followed by the addition of a solution of PAA (20 g) in 50 mL of water. The reactor was sealed and

heated at 200 °C for 24 h. After cooling of the reactor to room temperature, CFs were separated, washed 5 times with deionized water and dried for 12 h at 80 °C.

- In the presence of sodium oleate as a capping agent (sample ID: CF-hydro-NaOleate): rCFs were placed in a reactor, and subsequently a solution of $FeCl_2\cdot 4H_2O$ (15.8 g) and $FeCl_3\cdot 6H_2O$ (37.8 g) in 70 mL deionized and deoxygenated water (N_2 purged) was added. Following this, ammonia solution (28%, 150 g) was added, and then a solution of sodium oleate (5.95 g) in 50 mL of water. The reactor was sealed and heated at 200 °C for 24 h. After cooling of the reactor to room temperature, CFs were separated, washed 5 times with deionized water and dried for 12 h at 80 °C.
- In the presence of PEG as a capping agent (sample ID: CF-hydro-PEG): rCF were placed in a reactor, a solution of $FeCl_2\cdot 4H_2O$ (15.8 g) and $FeCl_3\cdot 6H_2O$ (43.2 g) in 100 g of deionized water and 100 g of absolute ethanol was added. Afterwards, PEG-400 (20 mL) was dispersed in the solution, and NaOH was added drop-by-drop to obtain a pH of around 10. Then, the reactor was sealed and heated at 180 °C for 16 h. After cooling of the reactor to room temperature, CFs were separated, washed 5 times with deionized water and dried for 12 h at 80 °C.

2.2.3. Characterization Methods

The optical microscope used for the characterization of reclaimed and functionalized CFs was the Zeiss Axio Imager 2, with AxioVision software, under a magnification of ×5 to ×100. A neodymium magnet (cylinder with a diameter of 10 mm, thickness of 2 mm and axial magnetization direction, grade N30) was used for an initial characterization of the magnetic behaviour of the nanocomposites created. X-ray powder diffraction (XRD) was carried out on a Bruker D8 Advance diffractometer with Cu-Kα radiation (Bruker, Cartenet, NJ, USA) to identify the crystalline structure of the synthesized magnetic nanoparticles. The morphology and the elemental analysis of the samples were determined by scanning electron microscopy (SEM) and energy-dispersive X-ray spectroscopy (EDS) using a PHILIPS Quanta Inspect (FEI Company, Hillsboro, OR, USA) microscope with a W (tungsten) filament 25 kV equipped with Edax Genesis (Ametek Process & Analytical Instruments, Pittsburg, PA, USA).

For the induction heating experiments, the radio frequency (RF) generator TruHeat HF 5010 (Trumpf Hüttinger, Freiburg, Germany) was used to generate an alternating magnetic field. The RF specifications considered a maximum power of 10 kW, maximum current of 35 A and input voltage of 600 V, including capacitors for operating at frequencies of 325 kHz, 436 kHz and 575 kHz. The water-cooled coil was a solenoid type with six turns, an internal diameter of 4.5 cm and a length of 8.5 cm. Samples were placed in the centre of the coil and exposed to a generated magnetic field, and the temperature increase was monitored using a thermo-camera FLIR E5 at distance of 30 cm (see Figure 2).

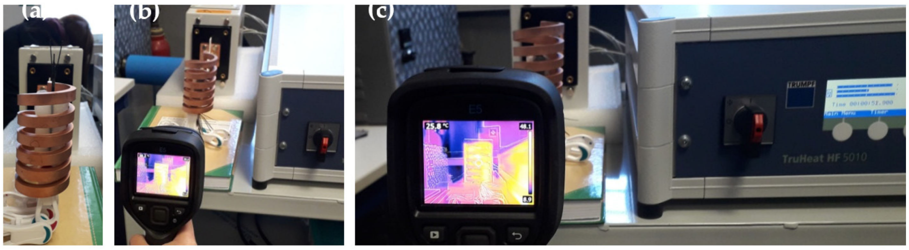

Figure 2. Induction heating equipment: (**a**) solenoid coil (including a sample inside), (**b**,**c**) RF Generator TruHeat HF 5010 set up with external circuit, coil and thermo-camera.

Sample preparation for induction heating testing: reclaimed and functionalized CFs were embedded in a polypropylene (PP) matrix and moulded as a cuboids with dimensions of 80 mm length, 15 mm width and 5 mm thickness (Figure 3). The PP cuboid containing functionalized rCFs was then placed in the centre of the solenoid coil and exposed to the electromagnetic field.

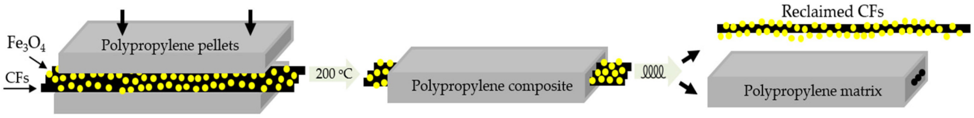

Figure 3. Schematic presentation of polypropylene composite specimens' preparation for induction heating experiments and CF reclamation after exposure to the magnetic field.

3. Results and Discussion

3.1. General Aspects

The results are compiled in Tables 2–4, followed by observations.

Table 2. General aspects of samples after reactions.

Sample ID	Control Sample	CF-hydro-nocoating	CF-hydro-PAA	CF-hydro-PAA-long	CF-hydro-NaOleate
Sample picture	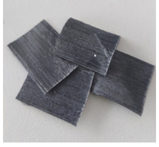	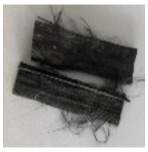			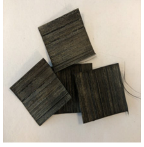
Sample ID	CF-hydro-PEG	CF-sc-CO_2	CF-dep-acetone	CF-dep-acetone-long	CF-dep-EtOH
Sample picture				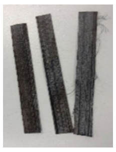	

Table 3. Optical microscopy (OM) images of non- and functionalized CF samples; magnification ×225.

Experiment	Control Sample	CF-hydro-nocoating	CF-hydro-PAA	CF-hydro-PAA-long	CF-hydro-NaOleate
OM image	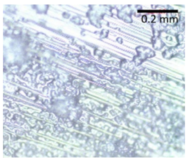	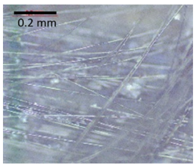	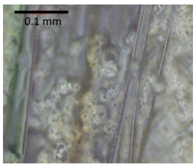	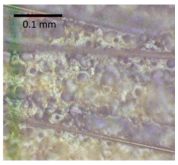	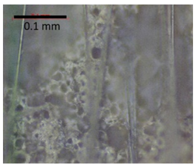
Experiment	CF-hydro-PEG	CF-sc-CO_2	CF-dep-acetone	CF-dep-acetone-long	CF-dep-EtOH
OM image	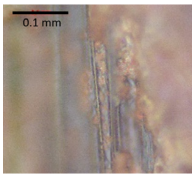	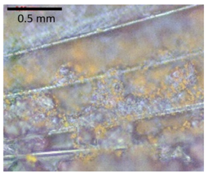	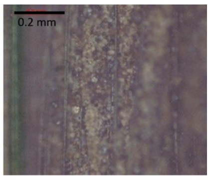	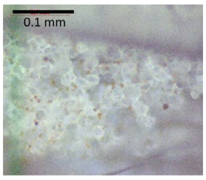	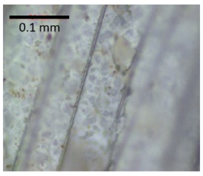

Table 4. Magnetic behaviour of samples.

Experiment	**CF-hydro-nocoating**	**CF-hydro-PAA**	**CF-hydro-PAA-long**	**CF-hydro-NaOleate**	**CF-hydro-PEG**	**CF-sc-CO_2**	**CF-dep-acetone**	**CF-dep-acetone-long**	**CF-dep-EtOH**
Magnetism of sample	No	Yes (strong) see Section 3.4	Yes (strong)	Yes (weak)	No	No	Yes (strong) see Section 3.4	Yes (weak)	Yes (weak)
Magnetism of particles in solution	Yes	Yes	Yes	Yes	No	No	Yes	Yes	Yes

The CFs obtained from CF-hydro-nocoating experiment were brittle, and particles were not observed on their surface. After the CF-hydro-PAA and CF-hydro-PAA-long (hydrothermal synthesis with PAA surfactant) experiments, a grey colour appeared at the surface of rCF. For CF-hydro-NaOleate treated CFs (hydrothermal reaction with sodium oleate surfactant), a grey colour appeared that was more accentuated than after CF-hydro-PAA treatment. After the CF-hydro-PEG experiment (hydrothermal reaction with PEG400 as surfactant), a red colour was present at the surface of the rCF. For the CF-sc-CO_2 experiment (sc-CO_2 synthesis), the sample presented a bluish reflection at the surface, and the fibres were covered with red coloured particles. After the CF-dep-acetone and CF-dep-acetone_long trials (deposition of NP in acetone and sc-CO_2), samples were damaged, fibres were less bonded than before the treatment, and deposition of brown-grey particles appeared at the surface of rCF. For the CF-dep-EtOH experiment (deposition of NP in ethanol and sc-CO_2), the samples remained in the usual (pre-preg like) shape, and a grey layer of material was observed at the surface of rCF.

Following various surface treatments, all rCF samples showed experiment-specific modification. In addition, different results from some trials, i.e., CF-hydro-PEG and CF-sc-CO_2, were obtained, demonstrating that the treatment of CFs under different synthesis conditions may lead to the generation of particles of different natures.

3.2. Mesoscopic Aspects

For the CF-hydro-nocoating, there is no visible difference between the treated and untreated samples as observed by optical microscopy (Table 2), except for the damages observed on the surface of treated CFs. For the control sample, black microparticles were present at the surface of fibres, which represent the remaining epoxy matrix of recycled prepreg. For CF-hydro-PAA and CF-hydro-PAA_long, agglomerations of dark-brown particles can be observed at the surface of rCF, apparently bonded with the remaining epoxy matrix. For CF-hydro-NaOleate, similar features can be observed, although the particles seem to be fewer in number than for CF-hydro-PAA. For CF-hydro-PEG, red particles are observed at the surface of rCF, mainly bonded with the polymer matrix. For CF-sc-CO_2 with rCF, microparticles are present at the surface of rCF, with an orange-like coloration. According to the microscopy images in Table 2, at the surface of samples of CF-dep-acetone, many microstructured features can be observed. They are similar to the microparticles of epoxy matrix visible on the control sample, but they have a brown colour, likely due to the presence of MNPs. On CFs after the CF-dep-acetone-long experiment, the particles seem to be fewer. For CF-dep-EtOH, images of the surface show a matrix, clearer than in the control sample, that is formed by agglomerated “melted” microparticles. Small red-brown spots can be seen in the grey matrix, but they are fewer in number than in CF-dep-acetone.

Except for the CF-hydro-nocoating, all the samples show the presence of particles visible by optical microscopy, with variations in concentration and colour.

3.3. Magnetic Behavior Aspect

The evaluation of magnetic behaviour of the sample and the particle in solution allowed us to estimate the degree of functionalization of the fibres and indicated if the particles synthesized are magnetic or not, to assess the success of the reaction. In the case of CF-hydro-nocoating, the particles in solution are magnetic but not the fibres, and it is assumed that their deposition on the CF surface failed. For CF-hydro-NaOleate, CF-dep-acetone_long and CF-dep-EtOH, the reaction of the sample to a magnet is weak, but the particles in solution had a good magnetic response; the assumption that can be made is that the deposition of MNPs is ineffective. For CF-hydro-PAA, CF-hydro-PAA-long and CF-dep-acetone, particles and fibres have a good magnetic response (Figure 4), a sign of significant deposition of magnetic particles. For CF-hydro-PEG and CF-sc-CO_2, neither the particle nor the fibres are magnetic; the synthesized brown particles are not pure Fe_3O_4 as expected.

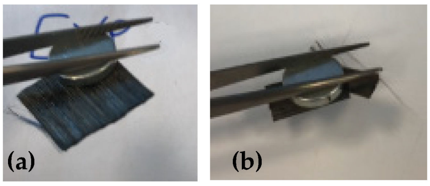

Figure 4. Magnetic response to magnet for (**a**) CF-hydro-PAA and (**b**) CF-dep-acetone.

In conclusion, the magnetic behaviour of samples and particles in solution was variable and showed that the functionalization of the fibres was not successful for all experiments; only CF-hydro-PAA and CF-dep-acetone seemed to have a good presence of MNP at their surface.

3.4. Microstructural Characterization

The remaining solutions from samples of CF-hydro-nocoating to CF-hydro-PEG were post-treated after the reaction to evaporate the solvent and collect the deposited powder for XRD analysis. CF-sc-CO_2 was excluded from the analysis due to insufficient material recovered from the solution. The obtained XRD patterns are presented in Figure 5. Dotted blue lines indicate the position of peaks at angles of 30.0° and 36.6°, corresponding to the planes (220), and (311) of Fe_3O_4. More dominant peaks were observed for different salts and other sub-products obtained for the synthesis, i.e., NH_4Cl and NaCl. Fe_3O_4 (magnetite) was detected in powders from CF-hydro-nocoating and CF-hydro-PAA. For CF-hydro-NaOleate, magnetite was detected as well as maghemite (γ-Fe_2O_3). For CF-hydro-PEG, the iron oxide detected was α-Fe_2O_3 (hematite). In conclusion, only samples CF-hydro-nocoating and CF-hydro-PAA appeared to have formed magnetite crystal structures.

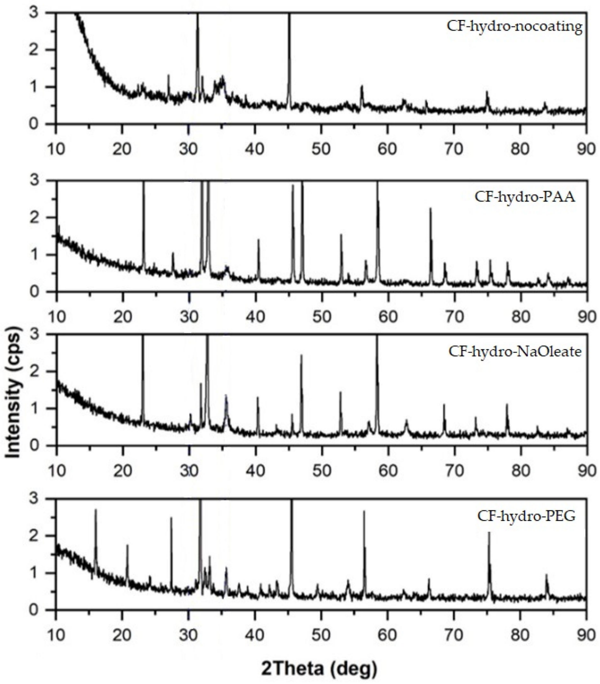

Figure 5. XRD spectra of samples, with zoom in Fe_3O_4 peaks.

3.5. NP Size, Morphology and Composition

The SEM analysis allowed us to understand more about the morphology of synthesized particles, whereas EDS provided their semiquantitative elemental composition. The results are compiled in Table 5. for the CF-hydro-nocoating sample, only a minor deposition of microclusters is noticed; EDS analysis on clusters present at the surface of rCF identified 3% wt of iron. For CF-hydro-PAA, the synthesized MNP forms clusters with a size between

150 and 400 nm, composed of MNP of about 20 nm, with a percentage of iron present at the surface at 39% wt. For CF-hydro-PAA_long, the presence of NP is significantly reduced, as was the quantity of iron (13% wt). For CF-hydro-NaOleate, the presence of polymeric residue at the surface of rCF renders the morphological assessment difficult due to the difficult distinction between polymeric residue and iron oxide species possibly formed on the surface of the fibres. Nevertheless, a minor percentage of iron is exhibited in the elemental analysis (1% wt). For CF-hydro-PEG, a deposition is presented between the fibres, clustering in micrometre size, with the presence of iron (about 11% wt). The sample CF-sc-CO_2 exhibits large growth of material on the surface of the fibres as well as spherical particles in the micrometre scale (diameter between 0.5 and 3 µm). In larger magnification, the microparticles seem to emerge from the material that engulfs the CFs. EDS results show an important iron percentage (70% wt).

Table 5. SEM pictures of samples and % wt of iron measured with EDS.

Experiment	Control Sample	CF-hydro-nocoating	CF-hydro-PAA	CF-hydro-PAA- long	CF-hydro-NaOleate
image	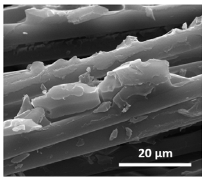	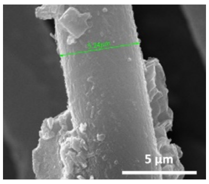	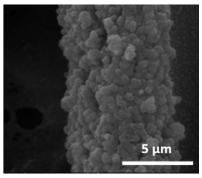	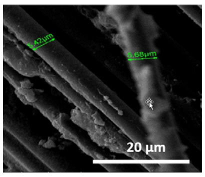	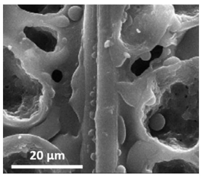
% of iron	/	3	40	13	1
Experiment	CF-hydro-PEG	CF-sc-CO_2	CF-dep-acetone	CF-dep-acetone-long	CF-dep-EtOH
image	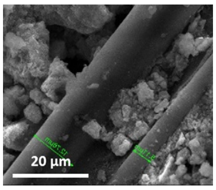	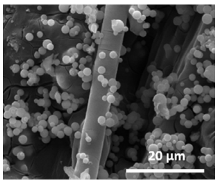	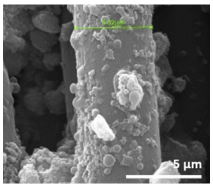	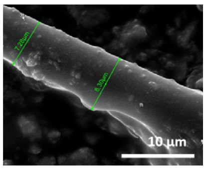	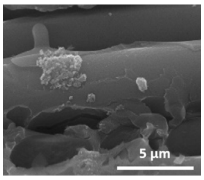
% of iron	11	70	39	4	8

Regarding the deposition experiments, SEM/EDS analysis results for CF-dep-acetone indicated MNP present at a large scale at the surface of rCF, with a percentage of iron at 39% wt. The upscaling experiment with CF-dep-acetone_long showed a minor MNPs deposition, with a presence of iron at 4% wt. For CF-dep-EtOH, a minor presence of NP was seen at the surface of CF (8% wt of iron). Based on the results of SEM/EDS analysis, samples of CF-hydro-PAA and CF-sc-CO_2 were successfully functionalized with iron oxide in comparison with the rest of the samples, which exhibited medium or minor deposition. In addition, these results are in agreement with the XRD analysis and the magnetic assessment. It should be noted that for all experiments, no degradation of CF was observed with SEM; the surface was smooth, and the diameter was about 5.5 µm. All the results of different characterizations are compiled in Table 6.

Table 6. Summary of characterization results.

Sample ID	**General Aspect**	**Mesoscopic Aspect**	**Magnetic Behaviour**	**Nature of Particles**	**Microscopic Aspect**	**% of Iron**
Control sample	grey	resin fragments	no	Fe_3O_4	resin residues on fibre	0
CF-hydro-nocoating	black, brittle	no particles	no	Fe_3O_4	minor deposition of clusters	3
CF-hydro-PAA	clear-grey	black particles	yes	Fe_3O_4	clusters covering the fibres	40

Table 6. *Cont.*

Sample ID	General Aspect	Mesoscopic Aspect	Magnetic Behaviour	Nature of Particles	Microscopic Aspect	% of Iron
CF-hydro-PAA-long	grey	black particles	yes	Fe_3O_4	deposition of clusters	13
CF-hydro-NaOleate	grey	black particles	weak	Fe_3O_4	resin residues on fibre	1
CF-hydro-PEG	reddish	red particles	no	Fe_2O_3	microclusters between fibres	11
CF-sc-CO_2	reddish	red particles	no	insufficient	spherical microparticles	70
CF-dep-acetone	clear-grey, brittle	brown particles	yes	Fe_3O_4	deposition of clusters	39
CF-dep-acetone-long	clear-grey, brittle	brown particles	weak	Fe_3O_4	minor deposition of clusters	4
CF-dep-EtOH	clear-grey	brown particles	yes (weak)	Fe_3O_4@oleic-acid	minor deposition of clusters	8

3.6. Evaluation of Heating Performance

After preliminary testing with a NdFeB magnet and elemental analysis of iron by EDS, CF-hydro-PAA_long was selected for testing to assess its response to alternating magnetic fields and its ability to produce hysteresis heating by deposited ferrimagnetic nanoparticles. Long functionalized CFs, obtained through a supercritical synthesis upscaled process, were embedded in a polypropylene (PP) matrix (melting temperature 180°) and then exposed to an electromagnetic field. The temperature distribution of the heated sample was measured using an IR camera and was recorded in 15 s time intervals.

The CF-hydro-PAA_long sample rapidly reached 145 °C in the first 15 s. Then, the temperature gradually increased to 177 °C in 5 min (Figure 6). The polymer matrix was heated, reaching the melting temperature of PP, enabling the triggering of magnetic nanoparticles to heat the polymer matrix and induce healing or separation/reclamation of CFs from the polymer in a melted state.

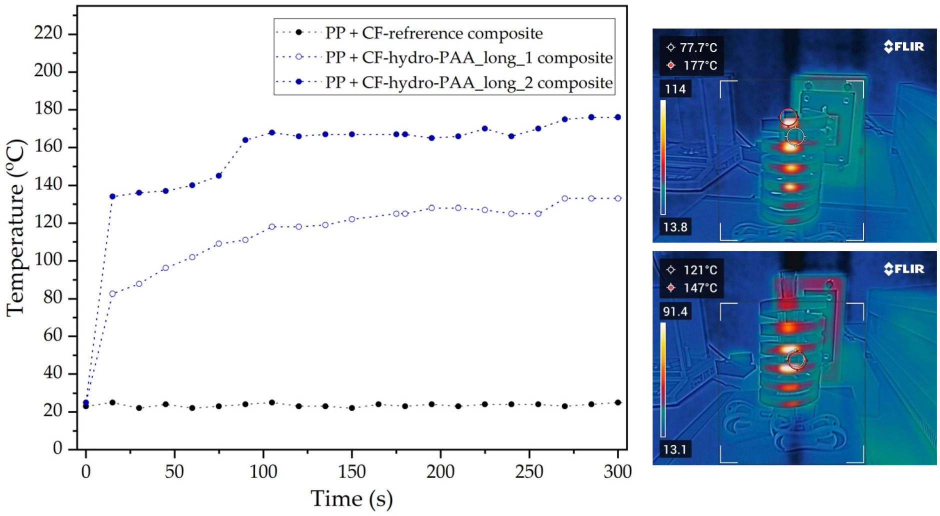

Figure 6. Induction heating of composite PP + CF-hydro-PAA_long: temperature is a function of time at the surface of a sample made on PP, integrating the CF-hydro-PAA_long sample inside (575 kHz, 6 kW). The picture shows the sample heating with an IR camera.

3.7. Discussion

The results in the previous sections demonstrated that different surface treatment approaches led to functionalization of CFs with various efficiencies: from less successful, due to the nature of particles created due to the lack of surface grafting of the nano and microparticles, to successful deposition of MNPs and functionalization of CFs.

On the CF sample in CF-hydro-nocoating, synthesis was realized without using a surfactant/capping agent [8], which allowed avoiding aggregation of magnetic nanoparticles. The deposition of particles is minor at the surface of CF, with irregular clusters and no sign of nanoparticle presence. The sample was not magnetic, but particles created in solution after the reaction were Fe_3O_4. The lack of deposition at the surface of CF could be the result of the aggregation of the Fe_3O_4 particles during the reaction. On CF sample in CF-hydro-PEG, the functionalization was present with MNPs at the micrometre size; most probably, the particles created were Fe_2O_3. In CF-sc-CO_2, iron-oxide spherical microparticles were synthesized and grafted at the surface of CF, though the sample and the particles in solution revealed a lack of magnetism.

The experiments involving CF-hydro-PAA, CF-hydro-NaOleate, CF-dep-acetone and CF-dep-EtOH were successful, with varying results in terms of efficiency of functionalization of CFs. In experiments involving CF-hydro-PAA and CF-hydro-NaOleate, the same reactants were used, with different surfactants tested: PAA (CF-hydro-PAA), which was hydrophilic, and sodium oleate (CF-hydro-NaOleate), with hydrophobic properties [10]. These experimental set-ups involved aqueous solutions of $FeCl_2 \cdot 4H_2O$ and $FeCl_3 \cdot 6H_2O$, with the addition of ammonia and functionalization of CFs in hydrothermal conditions (200 °C, sealed autoclave) for 24 h. CF-hydro-PAA exhibited Fe_3O_4 synthesis and a good functionalization of rCF. Long CFs were treated in the up-scaled CF-hydro-PAA process (the only change was the length of samples, CF-hydro-PAA_long) to prepare samples applicable for induction heating tests; however, the result was a minor functionalization in terms of deposited iron oxide. Nevertheless, the sample exhibited magnetic behaviour. The diminution of the presence of iron at the surface of CF for CF-hydro-PAA_long could be explained by the shape of the samples, which may have allowed a lower circulation of the fluids around and in the samples during the reaction. Regarding the induction response of CF-hydro-PAA-long, the ability of MNP at the surface of CF to heat was proven, reaching the melting point of PP; however, the heating was not sufficient to melt a larger area of the PP matrix around CFs to allow their reclamation. It appears that a good deposition was possible on rCF with hydrophilic particles, possibly because rCFs are composed of CF and polymeric residues, which possess -OH and -COOH hydrophilic functional groups, allowing a covalent bonding between rCF and hydrophilic capped particles. CF-hydro-PAA is a promising experimental set-up, with strong magnetism and good functionalization; this would be interesting to explore in the context of the simultaneous process of functionalization of rCF after sc-CO_2 extraction. The use of a larger reactor could improve the circulation of fluids during the reaction, allowing a better functionalization for long samples.

CF-dep-acetone and CF-dep-EtOH show an innovative process of deposition of already synthesized NPs, using sc-CO_2 to allow the transport of NP inside rCFs. Two different co-solvents used to solubilize oleic-acid-capped MNPs were tested: acetone (CF-dep-acetone) and ethanol (CF-dep-EtOH). The results show a very good deposition of NPs with acetone as a co-solvent, and a good magnetic response of the samples. The results were not promising for CF-dep-EtOH samples (with ethanol as cosolvent), with a weak magnetic response of the samples, and a minor presence of NP noted at the surface of CF. The differences between these two experiments can be attributed to the reaction of acetone in the epoxy matrix during the deposition, which dissolved an important part of the thermosetting resin, allowing the NPs to further penetrate into the fibres than for CF-dep-EtOH, where ethanol did not have this effect on the organic matrix.

CF-dep-acetone produced rCF functionalized with MNP, with strong magnetism; this seems to be a way to complete the recycling process with rCF functionalization. Regarding the results in terms of functionalization and magnetism, the experimental set-up used for CF-dep-acetone was upscaled as for CF-hydro-PAA (the only change was the length of samples) to make the induction test samples, and the result of CF-dep-acetone-long was a weak functionalization compared to CF-dep-acetone, in correlation with its weak magnetic response. It appears that the shape of the samples has an important influence on the capability to transport NP with sc-CO_2 between the fibres; the circulation of supercritical fluid may be lowered with longer samples in the reactor. The induction response of CF-dep-acetone_long corresponds to the weakness of the deposition, with no increase in the temperature of the sample during the exposure to the electromagnetic field. As for CF-hydro-PAA, the experiment could be improved using a larger reactor to allow a better circulation of fluids and an improved deposition for longer samples.

4. Conclusions

Different experimental approaches were conducted to perform CF functionalization with MNPs by SCF chemistry after recycling, to ensure a simultaneous process between recycling and functionalizing. Two experimental approaches successfully functionalized rCF with Fe_3O_4 NP: (i) direct synthesis of MNPs on the CF surface under the hydrothermal conditions with PAA as a surfactant (see CF-hydro-PAA in Section 3.1) and (ii) the deposition of already-formed MNPs dispersed in acetone in sc-CO_2 media. Further optimization of procedures is required for up-scaling.

PP composites reinforced by functionalized rCFs were tested for local heating triggered by contactless induction heating and CF reclamation. It was demonstrated that functionalization of CFs with Fe_3O_4 nanoparticles enables magnetic induction heating via the magnetic hysteresis loss mechanism. The functionalization of recycled prepreg with magnetite nanoparticles coated with PAA through hydrothermal synthesis (CF-hydro-PAA_long) was sufficient to obtain rapid heating of rCF, reaching locally, in the area surrounding CFs, the melting point of PP, though not sufficient to heat whole composite samples and enable their reclamation/separation from thermoplastic matrix. It is expected that the composites with higher functionalized CFs-to-polymer volume ratio would allow reclamation. For CF-dep-acetone_long, the experimental set-up must be further improved for successful functionalization and a higher heating capacity of the composite PP/rCF by induction. A study of the durability of such functionalization of rCF, with an assessment of the fibre reclamation efficiency from a polymer matrix, should be performed to validate technology.

The demonstrated recycling process of UD-prepreg by sc-CO_2 [2] with a CF functionalization step can be further improved, to produce MNP-functionalized rCF, especially with the CF-hydro-PAA experimental set-up. The complete process includes: (i) recovering of uncured prepreg wastes from industrial manufacturers; (ii) cutting to obtain the desired size of CF; (iii) a CF extraction phase performed with an sc-CO_2 batch extractor; (iv) the functionalization with an MNPs phase (CF-hydro-PAA or CF-dep-acetone setup); (v) recovery of functionalized rCF ready for compounding or reuse.

Author Contributions: Conceptualization, S.M. (Sophie Martin) and S.M. (Sandy Moisan); methodology, S.M. (Sandy Moisan), validation, S.M. (Sandy Moisan) and T.K.M.; formal analysis, S.M. (Sandy Moisan); investigation, S.M. (Sandy Moisan); data curation, T.K.M.; writing—original draft preparation, S.M. (Sophie Martin); writing review and editing, T.K.M.; supervision, C.A.C.; project administration, C.A.C.; funding acquisition, C.A.C. All authors have read and agreed to the published version of the manuscript.

Funding: This work is funded by the European Union's Horizon 2020 research and innovation program, entitled: 'Recycling and Repurposing of Plastic Waste for Advanced 3D Printing Applications' (Repair3D) under GA No. 814588.

Data Availability Statement: Data sharing is not applicable.

Acknowledgments: The authors would like to express thanks to Afroditi Ntziouni and Maria Kanidi from NTUA for carrying out XRD and part of the induction heating experiments, and Airbus Nantes Plant for providing the prepregs.

Conflicts of Interest: The authors declare no conflict of interest.

References

1. Anastas, P.; Eghbali, N. Green Chemistry: Principles and Practice. *Chem. Soc. Rev.* **2010**, *39*, 301–312. [CrossRef] [PubMed]
2. Martin, S.; Guriec, H.P.; Moisan, S. Novel Method For Unpolymerized Prepreg Recycling Using Supercritical CO_2 Extraction. In Proceedings of the 20th European Conference on Composite Materials—Composites Meet Sustainability, Lausanne, Switzerland, 26–30 June 2022; Volume F, pp. 133–140. [CrossRef]
3. Yoonessi, M.; Lerch, B.A.; Peck, J.A.; Rogers, R.B.; Solá-Lopez, F.J.; Meador, M.A. Self-Healing of Core–Shell Magnetic Polystyrene Nanocomposites. *ACS Appl. Mater. Interfaces* **2015**, *7*, 16932–16937. [CrossRef] [PubMed]
4. Ahmed, A.; Ramanujan, R. Curie Temperature Controlled Self-Healing Magnet–Polymer Composites. *J. Mater. Res.* **2015**, *30*, 946–958. [CrossRef]
5. Corten, C.C.; Urban, M.W. Repairing polymers using oscillating magnetic field. *Adv. Mater.* **2009**, *21*, 5011–5015. [CrossRef] [PubMed]
6. Ramajo, L.A.; Cristobal, A.A.; Botta, P.M.; Porto Lopez, J.M.; Reboredo, M.M.; Castro, M.S. Dielectric and Magnetic Response of Fe_3O_4/Epoxy Composites. *Compos. Part A Appl. Sci. Manuf.* **2009**, *40*, 388–393. [CrossRef]
7. Hergt, R.; Dutz, S.; Röder, M. Effects of Size Distribution on Hysteresis Losses of Magnetic Nanoparticles for Hyperthermia. *J. Phys. Condens. Matter Inst. Phys. J.* **2008**, *20*, 385214. [CrossRef]
8. Mizutani, N.; Iwasaki, T.; Watano, S.; Yanagida, T.; Tanaka, H.; Kawai, T. Effect of ferrous/ferric ions molar ratio on reaction mechanism for hydrothermal synthesis of magnetite nanoparticles. *Bull. Mater. Sci.* **2008**, *31*, 713–717. [CrossRef]
9. Haw, C.Y. Hydrothermal synthesis of magnetite nanoparticles as MRI contrast agents. *Ceram. Int.* **2010**, *36*, 1417–1422. [CrossRef]
10. Kolen'ko, Y.V. Large-Scale Synthesis of Colloidal Fe_3O_4 Nanoparticles Exhibiting High Heating Efficiency in Magnetic Hyperthermia. *J. Phys. Chem. C.* **2014**, *118*, 8691–8701. [CrossRef]
11. Kumar, P.; Khanduri, H.; Pathak, S.; Singh, A.; Basheed, G.A.; Pant, R.P. Temperature Selectivity for Single Phase Hydrothermal Synthesis of PEG-400 Coated Magnetite Nanoparticles. *Dalton Trans.* **2020**, *49*, 8672–8683. [CrossRef]
12. Hu, X.; Ma, M.; Zeng, M.; Sun, Y.; Chen, L.; Xue, Y.; Zhang, T.; Ai, X.; Mendes, R.G.; Rümmeli, M.H.; et al. Supercritical Carbon Dioxide Anchored Fe_3O_4 Nanoparticles on Graphene Foam and Lithium Battery Performance. *ACS Appl. Mater. Interfaces* **2014**, *6*, 22527–22533. [CrossRef] [PubMed]
13. Zhang, L.; Ni, Q.-Q.; Natsuki, T.; Fu, Y. Carbon Nanotubes/Magnetite Hybrids Prepared by a Facile Synthesis Process and Their Magnetic Properties. *Appl. Surf. Sci.* **2009**, *255*, 8676–8681. [CrossRef]
14. Yu, R.; Jiang, C.-F.; Chu, W.; Ran, M.-F.; Sun, W.-J. Decoration of CNTs' Surface by Fe_3O_4 Nanoparticles: Influence of Ultrasonication Time on the Magnetic and Structural Properties. *Chin. Chem. Lett.* **2017**, *28*, 302–306. [CrossRef]
15. Wu, Y. Magnetite/Carbon Nanotubes Nanocomposite: Facile Hydrothermal Synthesis and Enhanced Cycling Performance and High-Rate Capability as Anode Material for Lithium-Ion Batteries. *Ionics* **2015**, *21*, 635–643. [CrossRef]
16. Zhang, G.; Sun, S.; Yang, D.; Dodelet, J.-P.; Sacher, E. The Surface Analytical Characterization of Carbon Fibers Functionalized by H_2SO_4/HNO_3 Treatment. *Carbon* **2008**, *46*, 196–205. [CrossRef]
17. Wang, L.; Zhuo, L.; Zhang, C.; Zhao, F. Supercritical Carbon Dioxide Assisted Deposition of Fe_3O_4 Nanoparticles on Hierarchical Porous Carbon and Their Lithium-Storage Performance. *Chem. Eur. J.* **2014**, *20*, 4308–4315. [CrossRef]
18. Torque Magnetometers Brochure. Available online: https://qd-uki.co.uk/wp-content/uploads/2019/07/EZ-VSM-Brochure.pdf (accessed on 22 May 2023).
19. Chomchoey, N.; Bhongsuwan, D.; Bhongsuwan, T. Magnetic Properties of Magnetite Nanoparticles Synthesized by Oxidative Alkaline Hydrolysis of Iron Powder. *Kasetsart J. Nat. Sci.* **2010**, *44*, 963–971.
20. Tao, K.; Dou, H.; Sun, K. Interfacial Coprecipitation to Prepare Magnetite Nanoparticles: Concentration and Temperature Dependence. *Colloids Surf. Physicochem. Eng. Asp.* **2008**, *1–3*, 115–122. [CrossRef]
21. Kennedy, R.J.; Stampe, P.A. Fe_3O_4 films grown by laser ablation on Si (100) and GaAs (100) substrates with and without MgO buffer layers. *J. Phys. D Appl. Phys.* **1999**, *32*, 16–21. [CrossRef]
22. Si, S.F.; Li, C.H.; Wang, X.; Yu, D.P.; Peng, Q.; Li, Y.D. Magnetic Monodisperse Fe_3O_4 Nanoparticles. *Cryst. Growth Des.* **2005**, *5*, 391–393. [CrossRef]
23. Goya, G.F.; Berquó, T.S.; Fonseca, F.C.; Morales, M.P. Static and Dynamic Magnetic Properties of Spherical Magnetite Nanoparticles. *J. Appl. Phys.* **2003**, *94*, 3520–3528. [CrossRef]
24. Tang, X.; Wang, S.; Xu, D.; Gong, Y.; Zhang, J.; Wang, Y. Corrosion Behavior of Ni-Based Alloys in Supercritical Water Containing High Concentrations of Salt and Oxygen. *Ind. Eng. Chem. Res.* **2013**, *52*, 18241–18250. [CrossRef]
25. Lam, U.T.; Mammucari, R.; Suzuki, K.; Foster, N.R. Processing of Iron Oxide Nanoparticles by Supercritical Fluids. *Ind. Eng. Chem. Res.* **2008**, *47*, 599–614. [CrossRef]